Dual-Anode High-Pressure Xenon Cylindrical Ionization Chamber

Aleksey Bolotnikov, Alexander Bolozdynya, Raymond DeVito,
John Richards

Constellation Technology Corporation, 7887 Bryan Dairy Road,
Suite 100, Largo, FL33777-1498

Abstract **- A new approach to design of high-pressure xenon cylindrical ionization chambers is investigated. The dual-anode is used instead of a single anode surrounded with a shielding grid in the conventional design. Two coplanar anode wires are stretched near the axis of the chamber with a sensitive volume of 9 cm in diameter and 20 cm in length. Both the wires are kept at the same ground potential and DC-coupled to charge-sensitive preamplifiers. For the majority of the interactions, only one of the wires collects the electrons produced by ionizing particles. Both the wires detect the charge induced by uncollected positive ions. The difference between the signals read out from the wires is proportional to the charge of collected electrons. Absence of the grid makes the detector more robust, less sensitive to vibrations, and inexpensive. The first experimental results are compared to Monte Carlo simulations. The optimal chamber design is discussed.**

Index Terms **– xenon, ionization chamber, grid, spectrometer, gamma rays**

I. INTRODUCTION

Although proposed more than two decades ago [1-3], high-pressure (~50 bar) xenon (HPXe) ionization chambers received their long-deserved acknowledgement [4] only recently. Growing interest in HPXe detectors has been stimulated by the need for large-area, high-sensitivity, and robust detectors for non-destructive testing, nuclear treaty verification and safeguards, geological exploration and other industrial applications. To date, HPXe detectors represent a well-developed technique in gamma-ray detection [5-9]. Most of the technical problems that seemed unsolvable for decades have been overcome: purification of xenon gas, detector preparation, gas-filling and gas-handling procedure, and pressure effects influencing detector performance. Several designs of HPXe ionization detectors have been developed: parallel-plate, cylindrical and hemispherical chambers, TPC, and GSPC [5-15]. However, only cylindrical ionization chambers with a Frisch grid [16] have found practical uses and become commercially available [17]. This particular type of the chamber design has proven to be the most robust and cost effective and, at the same time, provides the best energy resolution (2% FWHM at 662 keV) due to a compensation effect of shielding inefficiency of the mesh. However, there is a severe drawback of these detectors: the shielding grid is very sensitive to mechanical vibrations and acoustic noise.

New detector designs without the shielding grid have been recently proposed to improve the performance of HPXe detectors [18-20]. The operational principle of these detectors is similar to the so-called coplanar-grid devices developed for room-temperature semiconductor detectors (see, e.g.,

Ref. [20]). However, the first tests of the new designs showed that direct copying of the coplanar-grid device design is not practical because of the high-level noise induced by the closely located differentially biased electrodes [19]. Moreover, the W-value in HPXe is about 20 eV: that is ~5 times higher than in room-temperature semiconductors. Thus, the signal-to-noise ratio in HPXe detectors is at least 5 times smaller, while the capacitances of the bulky electrodes in HPXe detectors are much larger than that of compact solid-state detectors. Thus, the induced low-frequency noise becomes an additional obstacle in large HPXe detectors with differentially biased co-planar electrode.

In this paper, we report on the first results of testing a novel HPXe detector with a dual-anode—a dual-anode cylindrical ionization chamber (DACIC)—which has non differentially biased anodes.

II. METHODS

A. Approach

In a new electrode design (see Fig.1), two anode wires replace a single anode surrounded by a grid normally used in conventional designs. Both wires are kept at zero potential. This is an important feature of our detector that makes it different from previously considered coplanar-grid devices [20]. For the majority of the events, only one wire (it can be either of the two) collects the electrons produced by the incident particles. The amplitude of the signal read from this wire is proportional to the number of the collected electrons minus the charge induced by uncollected positive ions. The signal induced by holes is the same for both wires. Thus, the signal difference between the two wires is proportional to the collected charge only.

Fig.2 (a,b) shows the electric-field lines distribution inside the chamber with the following geometrical parameters: the diameter of the each wire is 0.5 mm, the separation between the wires is 2 mm, and the cathode diameter is 100 mm. As is seen, in a large-scale (a) the electric-field lines distribution is symmetrical and similar to the field inside a single-anode cylindrical ionization chamber. The symmetry is broken only in the vicinity of the wires (b).

Fig. 3 (a,b) shows calculated pulse-shapes induced on both wires by a point-like charge as it drifts toward the anodes versus the initial location of the charge measured with respect to the center of the chamber for two cases: when the charge is located in a wires' plane (a), and the charge is located in a plane perpendicular to the wires' plane (b). The subtracted signals are also shown in Fig. 3 (a,b). In these calculations, an actual electric-field dependence of the electron drift velocity in HPXe was taken into account; a cathode bias of 20 kV was chosen. As is seen, in the case (a), the amplitude of subtracted signal is practically independent of the initial charge location, except for the area near the wires. In the other case (b), a slight amplitude dependence of the subtracted signal can be seen. This is due to a shielding effect of one wire by the other which makes the detector response asymmetrical. Several ways to overcome this problem will be discussed later. The straightforward solution is to select an optimal set of geometrical parameters for which the asymmetry in the detector response does not contribute more than 1% to the total energy resolution. In this work, we have chosen this approach as the simplest way to demonstrate the detector proof-of-concept.

The energy resolution of the DACIC device is determined by three major factors: intrinsic energy resolution of HPXe, electronic noise, and detector geometry. The latter affects the width of the peak in the detector's response function. Since the detector's response function is not symmetrical, the total energy resolution cannot be simply calculated as a sum of the above factors. We performed extensive Monte Carlo simulations to optimize the detector geometry. We found that the geometrical width of the response function becomes narrow when the smaller wire spacing is used. On the other hand, if the spacing is too small, the resolution can also degrade due to charge sharing between the anodes caused by electron diffusion in HPXe. For these reason, we chose a conservative approach and used a slightly larger spacing than optimal. We optimized a set of geometrical parameters for an expected electronic noise of 5 keV per channel. We found that, with a 3 mm spacing, a wire diameter of 0.7 mm, and a cathode diameter of 90 mm, the energy resolution at 662 keV gamma-line should be less than 2%. Fig. 4 (a) shows response functions simulated for these geometrical parameters and an electronic noise of 5 keV per channel.

DACIC can also be considered as a virtual-grid device with an effective grid that has a 100% transparency and does not perturb the electric field inside the chamber. In addition, the signal subtraction considerably reduces the microphone effect.

B. Detector design and electronics

To prove the concept, we chose the simplest detector design comprised of two parallel anode wires stretched in the middle of a ceramic tube whose inner wall surface was coated with an aluminum layer that served as a cathode (Fig.1). The diameter of the wires was 0.7 mm, length ~ 30 cm. The internal diameter of the ceramic tube was 90 mm. The distance between the centers of the wires was 3 mm. Both wires were held with two ceramic spacers mounted at the ends of the ceramic tube; for higher stability, small spacers were used to interconnect the wires in several places. The whole structure was mounted inside a high-pressure vessel and sealed with a Helicoflex gasket. The energy resolution of the DACIC device depends mainly on three factors: intrinsic resolution of HPXe, electronic noise, and detector geometry, which determines the width of the detector's response function. Since the detector's response function is not symmetrical, the total energy resolution cannot be simply calculated as a sum of the above factors. We performed extensive Monte Carlo simulations to optimize the detector geometry. We found that the geometrical width of the response function becomes narrow when the smaller anode spacing is used. On the other hand, if the spacing is too small the resolution can also degrade due to charge sharing between the two anodes caused by strong electron diffusion in the HPXe. For these tests, we chose a conservative approach and used a slightly larger spacing than optimal. Fig. 4 (b) shows response functions simulated for the geometrical parameters used in these measurements and the originally expected electronic noise of 5 keV per channel.

Two custom-made DC-coupled charge-sensitive preamplifiers with a ~5 ms decay time were used to read signals from the anodes. The signal subtraction was accomplished with a simple circuit consisting of two operational amplifiers similar to those developed for the coplanar-grid solid-state detectors [20]. The output signals were processed with standard spectroscopy electronics or digitized with a LeCrow Waveruner (LT 364L).

Since any of the wires may collect the charge, the output signal can be of both polarities: positive or negative. In this proof-of-concept work we ignored this effect and used only one anode wire for the collection electrons. This reduces the efficiency of the detector by a factor of two. To utilize signals of both polarities, digital pulse processing is required.

C. Gas purification

The assembled and sealed detector was baked under a vacuum of $<10^{-7}$ Tor for several days before filling with Xe. We used a spark purification technique to purify the Xe gas, whose purity level was monitored by measuring the electron lifetime (several milliseconds of electron lifetime). The Xe density was monitored by measuring a dielectric constant of HPXe as described elsewhere [12]. The density of the Xe used during these measurements was between 0.2 and 0.5 g/cm^3. A small admixture of hydrogen was added to the xenon to increase the mobility of the electrons. The typical collection time of electrons was 40-50 μs in pure Xe and ~15 μs in a Xe+H_2 mixture.

III. RESULTS DISCUSSION

We investigated two possible operation modes: (1) a single-anode mode, where the signals from the anodes were read out and evaluated independently, and (2) a dual-anode mode, where the two signals were subtracted each from the other.

A. Waveforms measurements

Figure 5 shows examples of waveforms induced by 662 keV photons from a ^{137}Cs gamma ray source used to generate the signals. The chamber was filled with pure Xe. As is seen, the shapes of the waveform are very similar to those theoretically calculated. The top positive waveform in every pair represents the "collected" signal read out from the anode that actually collected the electrons, while the bottom waveform represents the "induced" signals read from the second anode. The waveforms rise similarly until an ionization cloud approaches the anodes. In the vicinity of the anodes, the magnitude of the "collected" signal rapidly increases, while the magnitude of the "induced" signal rapidly drops and changes polarity representing the influence of the positive ions. This is easy to observe when the ionization cloud originated near the anodes (c). In these cases, when the interaction point is located near the cathode, the "induced" signal is positive (a). There are rare events when the charge is split between two anode wires (d) or when an incident photon produces two interaction points (b). By using digital pulse processing, all these events can be identified. Multi-point interactions are a common property of high-energy gamma rays. As is seen from Fig. 5, the distribution of the arrival time of the consequent electron clouds ranged in tens of microseconds, which requires a shaping amplifier with a long integration time.

B. Dual-anode mode

In the dual-anode operation mode, the signals read from the two anodes were subtracted from each other. We used two pulse-processing techniques to evaluate pulse-height spectra. We employed

a digital pulse-shaping technique when the chamber was filled with pure Xe. With pure Xe, the collection time is too long for commercially available shaping amplifiers. The original waveforms were digitized with the Waverunner within 200 μs time intervals (frames) with 400 ns resolution (500 points), and then digitally filtered with a shaping time of 40 μs. Low frequency analog filters were used to stabilize the baseline. Fig. 6(a) shows a pulse-height spectrum from a ^{137}Cs gamma source measured in the dual-anode mode. For comparison, Fig. 6(b) shows a spectrum measured at the same conditions from a single anode (single-anode mode). The data clearly demonstrates the advantage of the dual-anode operation mode over the single-anode mode at large shaping times in spite of the increased electronic noise caused by the two readout channels. We achieved a 26.5 keV (4.0%) FWHM energy resolution at 662 keV with electronic noise of ~13 keV per channel. The total electronic noise was measured with a test pulse generator to be 20 keV.

We used analog pulse processing when the chamber was filled with a Xe+H_2 mixture. The read out signals were first subtracted and shaped with a 20 μsec shaping time spectroscopy amplifier. The measured spectrum is shown in Fig. 7. Under these conditions, we obtained 4.2% FWHM energy resolution at 662 keV with a total electronic noise of 21 keV.

As was mentioned before, for these tests, we chose a conservative approach and used a slightly larger than optimal spacing. Fig. 4 (a,b) shows response functions simulated for the geometrical parameters used in these measurements and two levels of the electronic noise: actually measured 14 keV (a), and originally expected 5 keV (b). The predicted energy resolution in the case (a) is 3.9% at 662 keV, which is very close to the value actually measured. If we can improve the electronic noise per channel below 5 keV (which is a difficult task), we can expect a total energy resolution of <2% for the current chamber geometry.

C. Single-anode mode

The detector was tested in the single-anode operation mode in order to compare its performance with conventional single-anode cylindrical ionization chambers. Fig. 8 (a) shows a spectrum collected for the non-collimated ^{137}Cs source. The FWHM 662 keV peak measured at 6 μs shaping time is 3.0%. It should be emphasized that this is a very good result for the large volume high-pressure Xe detector without the shielding grid, e.g., this resolution is comparable to the best results obtained with "gridded" ionization chambers [20]. To illustrate the detector's capability to measure low energy gamma rays, Fig. 8 (b) shows a spectrum collected with a ^{57}Co source. The asymmetry of the 122 keV peak is due to the appearance of the ~90 keV escape peak.

The energy resolution of the DACIC operating in the single-anode mode is enhanced due to: (1) the presence of the second anode, which shares the charge induced by ions, and (2) the use of shorter amplifier shaping times, which helps to compensate for the slow rising portion of the signals. However, the short shaping time does not work in the cases of events with multiple interactions, whose probability increases with raising photon energy. As a result, the energy resolution degrades in the high-energy range. In order to compare the performance of the DACIC working in the single-anode and dual-anode modes, we acquired complicated spectra from a sample containing a natural mixture of Thorium isotopes (Fig. 9). One can see that the 2.6 MeV gamma ray peak totally disappeared from

the spectra acquired in the single-anode mode, but is very well resolved in the spectra measured in the dual-anode mode.

V. CONCLUSION AND DISCUSSION

The goal of this work was to evaluate the feasibility of a high-pressure ionization cylindrical chamber with a virtual Frish grid for precision gamma-ray spectrometry. The work was focused on proof-of-concept experiments of a cylindrical ionization chamber with an unbiased dual anode. Based on the results presented in this paper, the feasibility of the proposed approach was adequately demonstrated. It should be mentioned that the cylindrical geometry is an important feature of the DACIC that reduces a fraction of the charge sharing events in comparison with the parallel-plate geometry most often used in solid-state detectors.

The geometrical parameters of the chamber used in these measurements were not optimal, but dictated by other considerations described above. To achieve the theoretically expected energy resolution (~2% FWHM at 662 keV), we are planning to build a second version of the detector with improved electronics. By decreasing the spacing between the wire anodes to less than 2 mm, we expect less than 2% FWHM energy resolution with a realistic electronic noise of ~10 keV. To make the chamber geometry more symmetrical, one can stretch the wires at a small angle, or make a double helix by introducing special spacers between the wires. This also makes the whole anode structure more rigid. Another solution could be to shift the anodes off the center of the chamber. However, this would require the use of a cathode with axially distributed potential to compensate for electric-field distortions.

VI. ACKNOWLEDGEMENTS

The authors gratefully acknowledge the financial support of the DOE under SBIR Grant No. DE-FG0202ER83392. The authors thank Leo Godbee, Scott McPherson, and Ed Knighton for help in development of the instrumentation.

REFERENCES

[1] A.M. Galper, V.V. Dmitrenko, A.S. Romanuk and Z.M. Uteshev, The possibility of creation of high sensitive gamma-gay telescopes based on compressed Xe, 17th ICRC conference Papers 9, pp. 287-290, 1981.

[2] V.V. Dmitrenko, A.S. Romanuk, S.I. Suchkov, and Z.M. Uteshev, Electron mobility in high-pressure Xe, Journal of Technical Physics, Vol.53, p.2343 (1983). Translation in Sov. Phys.-Technical Phys., 28,1440 (1983).

[3] A.E. Bolotnikov, V.V. Dmitrenko, A.S. Romanuk, S.I. Suchkov and Z.M. Uteshev, Pribory I Tekhnika Eksperimenta, Vol.29, p.42 (1986) (USSR). Translation in Instr. and Exp. Tech., Vol.29, p.802 (1986).

[4] G.F. Knoll, Radiation Detection and Measurements, 3rd edition, John Wiley and Sons, pp.148-155, 2000.

[5] M.Z. Iqbar, B.M.G. O'Callaghan, and H.T. Wong, "Monte Carlo simulation of electron trajectories in high pressure xenon gas", Nucl. Instr. And Meth., A253, pp. 278-287, 1987.

[6] C. Levin, J. Germani and J. Markey, Nucl. Instr. and Meth., Vol. A332, pp.206-214 (1993).

[7] G. Tepper and J. Losee, A compressed xenon ionization chamber X-ray/gamma-ray detector incorporating both charge and scintillation collection, Nucl. Instr. and Meth., Vol. A368, pp.862-864, 1996.

[8] G.J. Mahler, B.Yu, G.C. Smith, W.R. Kane and J.R. Lemley, G. Smith, "A portable gamma-ray spectrometer for using compressed xenon", *IEEE Trans. Nucl. Sci.*, vol. NS-45, pp.1024-1033, 1998.

[9] A.E. Bolotnikov, V.M. Grachev, I.V. Chernesheva, V.V. Dmitrenko, A.M. Galper, S.V. Krivov, O.N. Kondakova, V.I. Lygushin, G.A. Shmatov, S.I.Suchkov, S.E. Ulin, Z.M.Uteshev, K.F. Vlasik, Yu.T. Yurkin, High-pressure Xe detector for gamma-ray astronomy onboard orbital station "Mir", Proc. of Intern. Conf. "Liquid Radiation Detectors: Their Fundamental Properties and Applications", Waseda University, Tokyo, Japan (ICLRD), 7-10 April 1992, p.462-465.

[10] Aleksey Bolotnikov and Brian Ramsey, Purification techniques and purity and density measurements of high-pressure Xe, Nucl. Instr. and Meth., Vol. A383, pp.619-623, 1995.

[11] A.E. Bolotnikov, V.V. Dmitrenko, A.S. Romanuk, S.I. Suchkov and Z.M. Uteshev, Electron-ion recombination on electron tracks in compressed xenon, Journal of Technical Physics, Vol.58, p.734, 1988. Translation in Sov. Phys.-Technical Phys., Vol.33, p.449, 1988.

[12] Aleksey Bolotnikov, Brian Ramsey, The spectroscopic properties of high-pressure xenon, Nucl. Instr. and Meth., Vol. A396, pp.360-370, 1997.

[13] S.E. Ulin, V.V. Dmitrenko, A.E. Bolotnikov, K.F. Vlasik, A.M. Galper, V.M. Grachev, I.V., O.N. Kondakova, V.B. Komarov, S.V. Krivov, S.V. Minaev, S.I.Suchkov, Z.M. Uteshev, Yu.T. Yurkin, I.V. Chernesheva, Cyllindrical high-pressure xenon detector of gamma-radiation, Instr. and Exp. Tech., Vol.37, n.2, pp.142-145, 1994.

[14] R. Kessick and G. Tepper, A hemispherical high-pressure xenon gamma radiation spectrometer, Nucl. Instr. and Meth, Vol. A490, pp.243-250, 2002.

[15] A. Bolozdynya, V. Egorov, et. al., High-pressure Xe self-triggered scintillation drift chamber with 3D sensitivity in the range of 20-140 keV, Nucl. Instr. And Meth. A 385, pp.225-238, 1997.

[16] Aleksey Bolotnikov and Brian Ramsey, Improving the energy resolution of high-pressure Xe cylindrical ionization chambers. IEEE Trans. Nucl. Sci., vol. 44, pp.1006-1010, 1997.

[17] A. Bolozdynya, A. Arodzero, and R. DeVito, "High-pressure xenon detectors for applications in portal safeguard systems and for monitoring nuclear waste", INMM 43rd Annual Meeting, Orlando, June 23-27, 2002.

[18] V.P. Miroshnichenko, B.U. Rodionov, and E. Shuvalova, Method of detection of gamma quanta, USSR patent SU-1264723A, issued on June 15, 1986.

[19] C.J. Sullivan, Z. He, G.F. Knoll, G. Tepper, and D.K. Wehe, A high pressure xenon gamma-ray spectrometer using a coplanar anode configuration. Nucl. Instr. And Meth. A 505, pp.238-241, 2003.

[20] P.N. Luke, Unipolar charge sensing with coplanar electrodes – application to semiconductor detectors. *IEEE Trans. Nucl. Sci*. v.42, n.4, pp.207-213, 1995.

FIGURE CAPTIONS

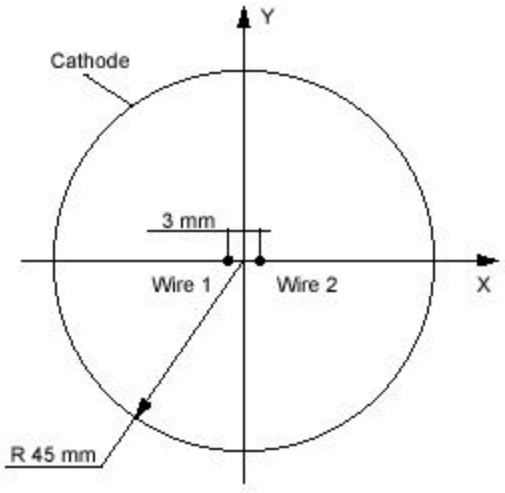

Fig.1. New electrode design for high pressure xenon ionization chamber

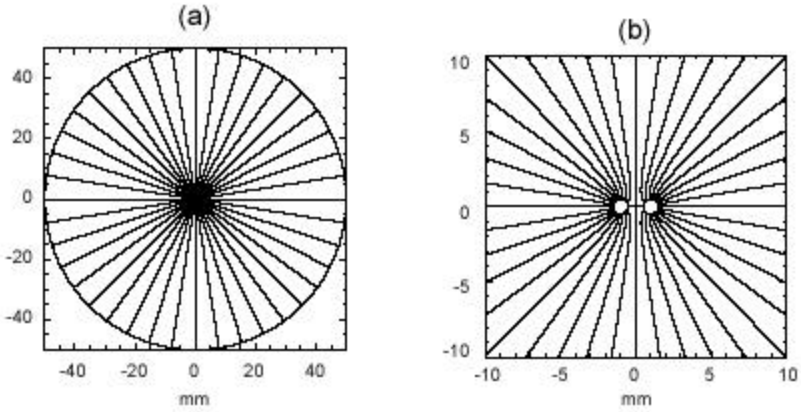

Fig.2(a,b). Electric field distribution in dual-anode cylindrical ionization chamber (a) and in vicinity of anodes (b).

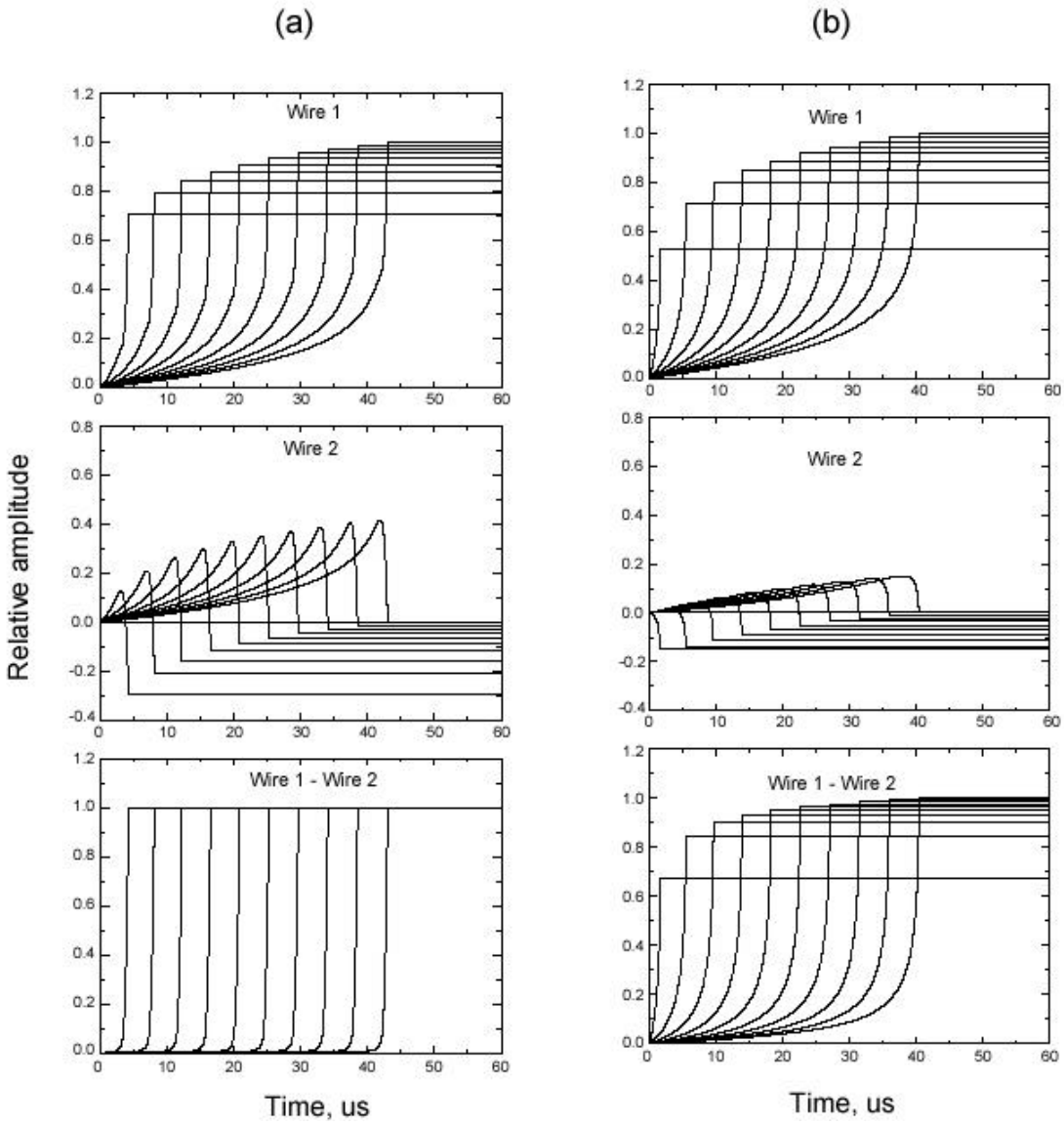

Fig.3(a,b). Calculated pulse-shapes induced on both wires by a point-like charge as it drifts toward the anodes versus the initial location of the charge measured from the center of the chamber for two cases: the charge is located in a wires' plane (a), and the charge is located in a plane perpendicular to the wires' plane (b).

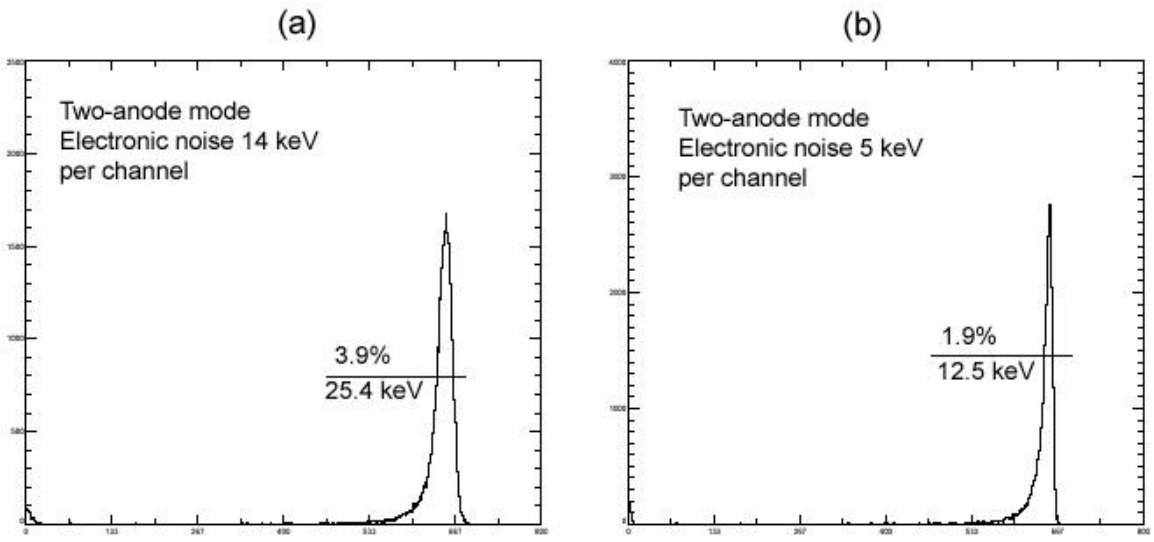

Fig. 4(a,b) Response functions simulated for the geometrical parameters of the chamber used in these measurements and two levels of the electronic noise: actually measured 14 keV (a), and originally expected 5 keV (b).

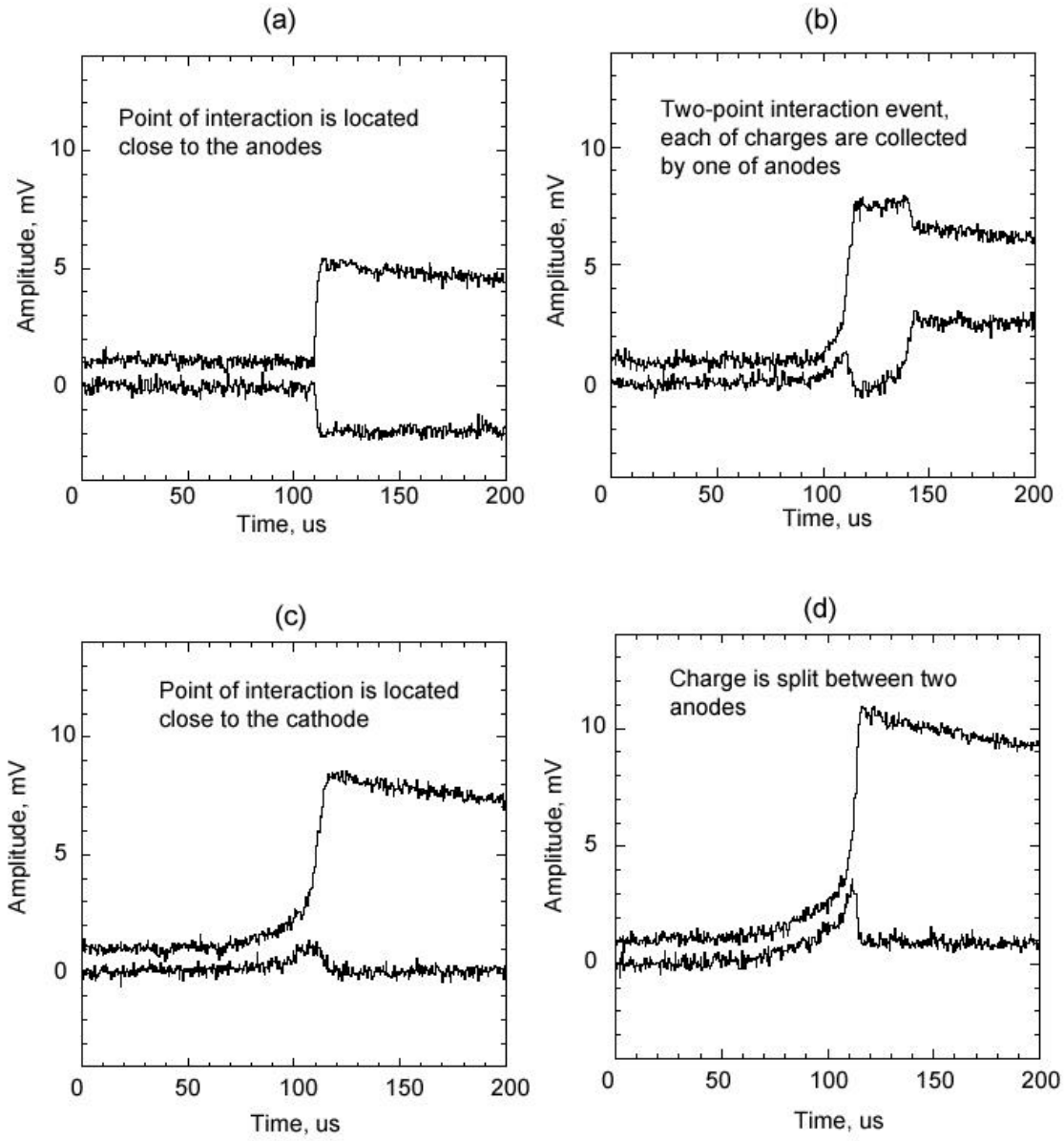

Fig.5. Examples of waveforms induced by 662 keV photons from a ^{137}Cs gamma ray source.

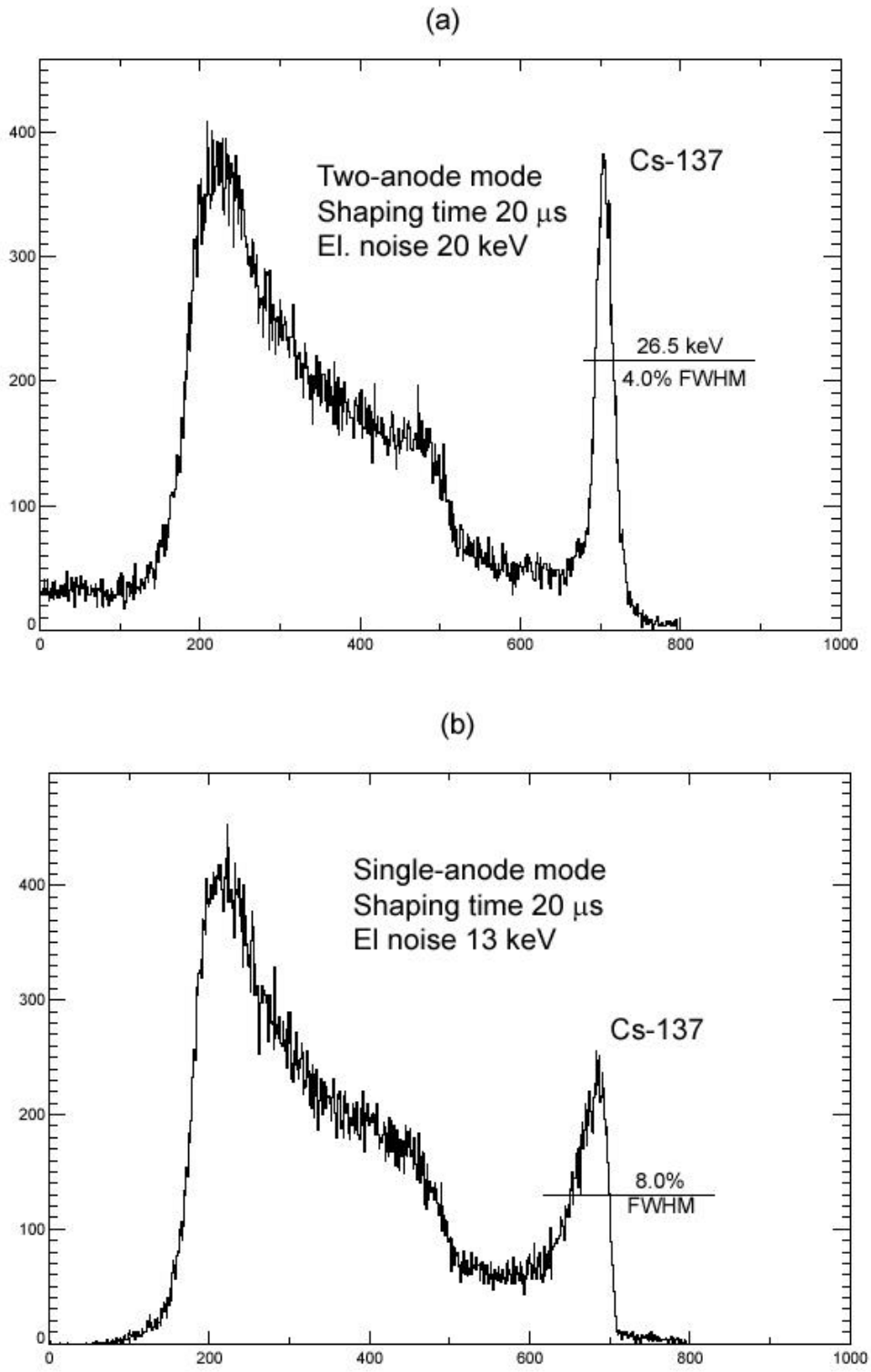

Fig. 6(a,b). Pulse-height spectra from a ^{137}Cs gamma-ray source measured for two modes: dual-anode (a) and single-anode (b). The chamber was filled with pure Xe. Digital pulse processing was used.

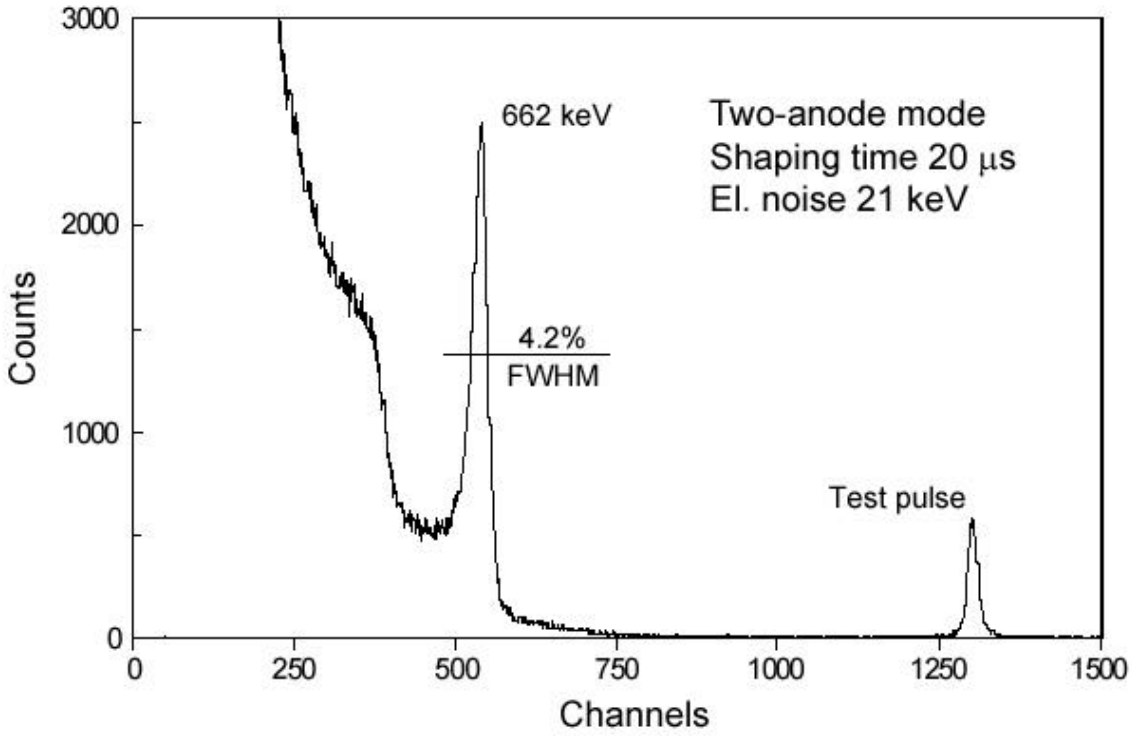

Fig. 7. Pulse-height spectrum from a ^{137}Cs gamma-ray source measured for dual-anode mode. The chamber was filled with $Xe+H_2$ mixture. Analog pulse processing was used.

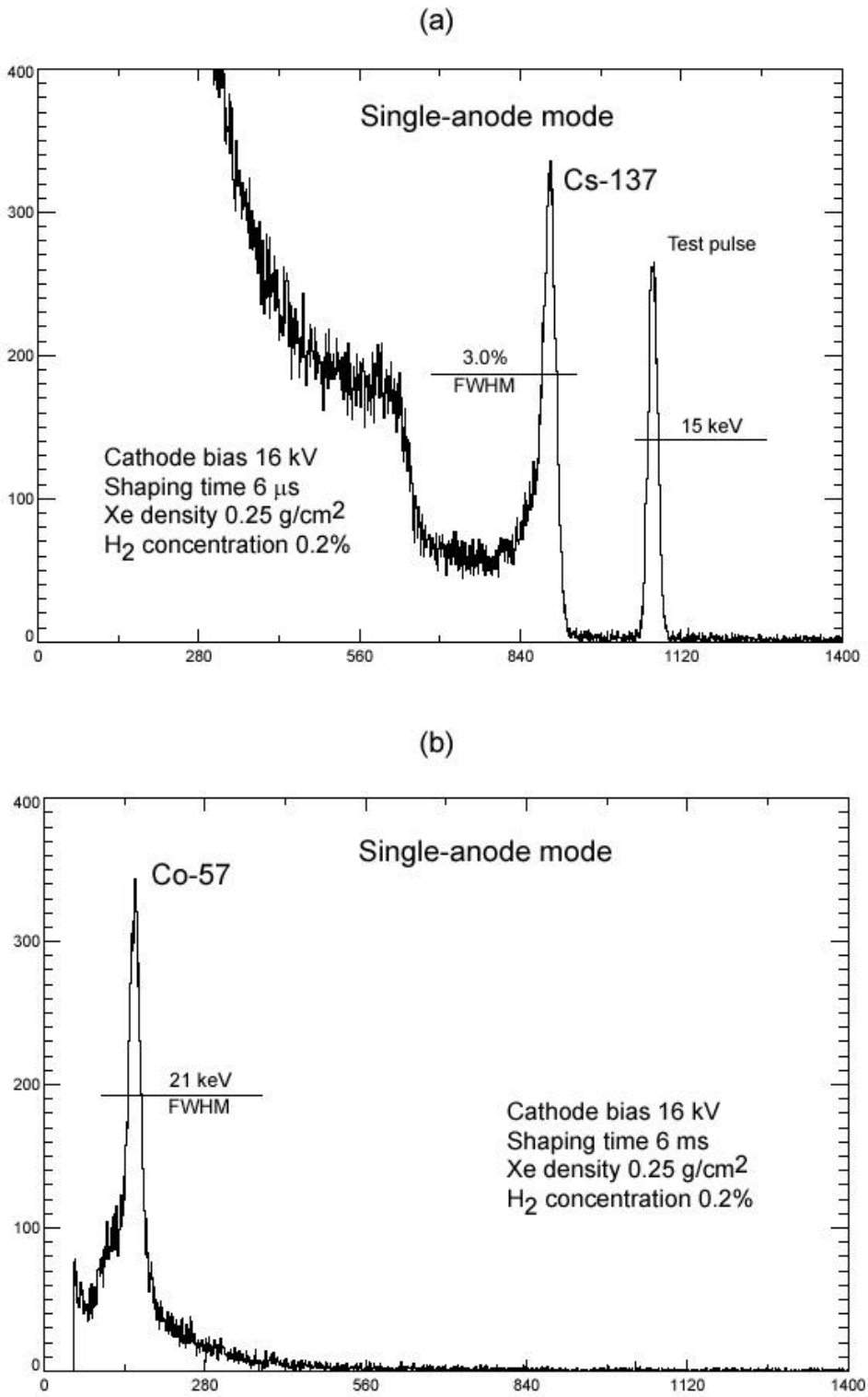

Fig. 8 (a,b). Pulse-height spectra measured with the uncollimated ^{137}Cs (a) and ^{57}Co (b) sources (single-anode mode).

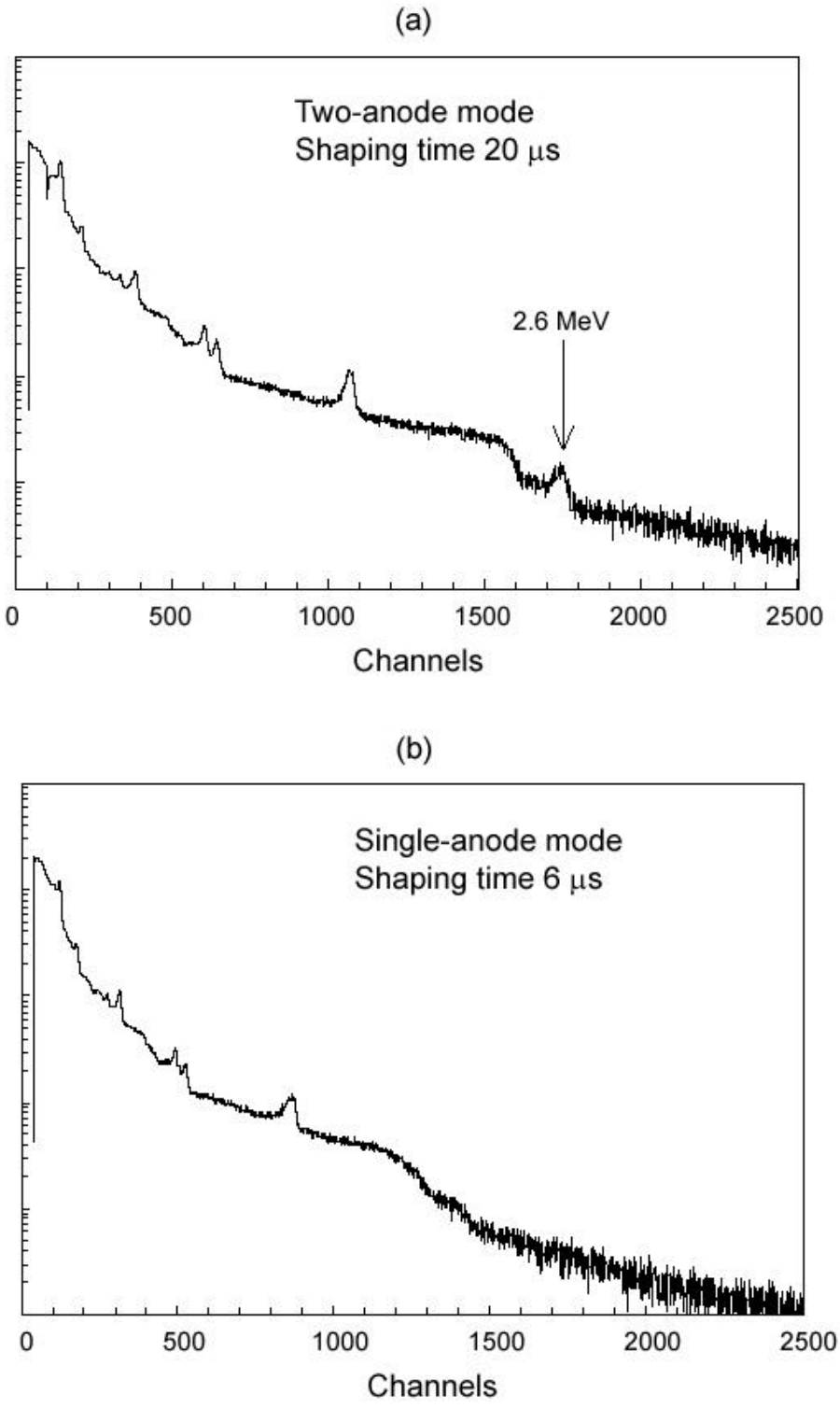

Fig. 9(a,b). Spectra from a sample containing a natural mixture of Thorium isotopes measured for two modes: dual-anode (a) and single-anode (b).